arXiv:1703.06050v1 [cond-mat.str-el] 17 Mar 2017

The role of the entropy in the ground state formation of magnetically frustrated systems within their quantum critical regime

Julian G. Sereni
Low Temperature Division, CAB-CNEA and Conicet, 8400 S.C. de Bariloche, Argentina
(Dated: March 20, 2017)

A systematic modification of the entropy trajectory ($S_m(T)$) is observed at very low temperature in magnetically frustrated systems as a consequence of the constraint ($S_m \geq 0$) imposed by the third law of thermodynamics. The lack of magnetic order allows to explore some unusual thermodynamic properties by tracing the physical behavior of real systems. The most relevant findings are: i) a common $C_m/T|_{T\to 0} \approx 7\,\mathrm{J/molK^2}$ 'plateau' in at least five Yb-based very-heavy-fermions (VHF) compounds; ii) quantitative and qualitative differences between VHF and standard non-Fermi-liquids. iii) Entropy-bottlenecks governing the change of $S_m(T)$ trajectories in a continuous transition into alternative ground states that exhibits third order characteristics. An empirical analysis of the possible $S_m(T \to 0)$ dependencies according to the $\partial^2 S_m/\partial T^2$ derivative is also preformed. Altogether, this work can be regarded as an empirical application of the third law of thermodynamics.

I. INTRODUCTION

The intensive study of the quantum critical (QC) behavior in heavy fermion (HF) compounds [1, 2] has powered the investigation of thermal properties in a significant number of new Ce and Yb intermetallics at $T \leq 1\,\mathrm{K}$. Despite of the unattainability of the $T = 0$ limit, the extremely low characteristic energies of these systems provide a fertile field to allow to perform an original test for the applicability of the third law of thermodynamics in real systems. As a consequence of this newly available information unpredicted behaviors of the thermal dependence of the entropy (S_m) have emerged in the thermal range where thermodynamic and QC fluctuations strongly interplay to stabilize the ground states of not ordered systems. These topics became recently relevant in the search for new materials suitable for adiabatic demagnetization refrigeration at the milikelvin range of temperature [3]

The usual magnetic behavior of Ce and Yb compounds can be properly described as a function of two coupling parameters [4, 5]: the inter-site RKKY magnetic interaction (J_R) and the on-site Kondo (J_K) interaction. As the local J_K coupling between band and localized $4f$ states increases, the intensity of the magnetic moments (μ_{eff}) decreases because of the Kondo screening. The consequent weakening of J_R ($\propto \mu_{eff}$) is reflected in the decrease of the magnetic order temperature (T_{ord}) that can be driven down to a QC point [6]. The different stages of this demagnetizing process as a function of J_K is schematically resumed in Fig. 1.

Once T_{ord} reaches the range at which thermal fluctuations compete with quantum fluctuations the QC scenario sets on (see the inset in Fig. 1). This regime is observed in heavy fermion (HF) compounds which behave as non-fermi-liquids (NFL) while approaching the QC regime [1, 2]. Once J_K overcomes J_R the Fermi Liquid (FL) behavior takes over. Within this regime the thermal ($\gamma = C_m/T$), magnetic (χ_0) and transport ($\rho = AT^2$) proportionality: $\gamma \propto \chi_0 \propto \sqrt{A} \propto m_{eff}$ is fulfilled, being m_{eff} the enhanced effective electron mass.

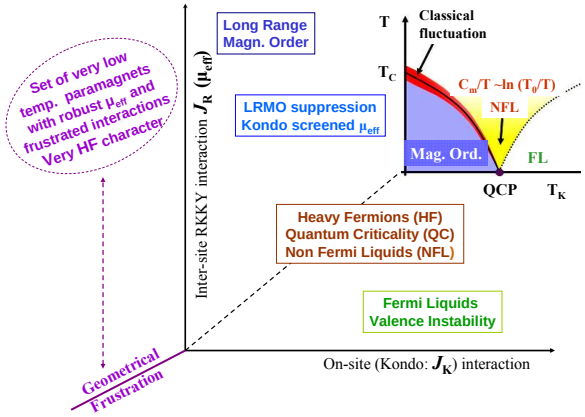

FIG. 1. (Color online) Schematic description of the magnetic behavior of Ce- (Yb-) lattice compounds as a function of two exchange parameters (see the text). The third axis represents frustrated (paramagnetic) systems. Inset: usual representation as a function of Kondo temperature. [4, 5].

There is, however, an increasing set of Ce and Yb compounds which escape for this description because they do not order magnetically despite of their robust μ_{eff} (i.e. $J_R \gg J_K$) in a lattice arrangement. This characteristic is mainly due to the frustration of an-

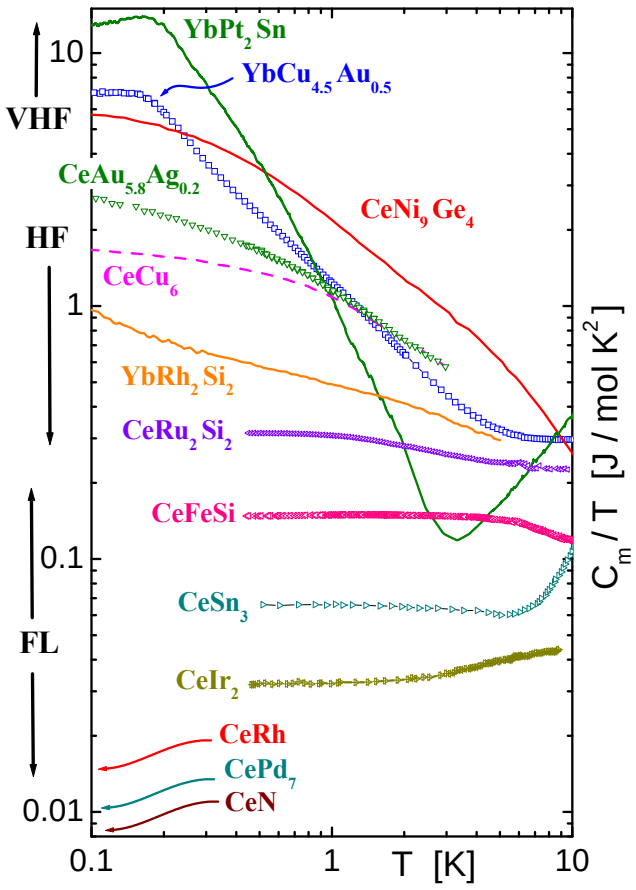

FIG. 2. (Color online) Examples of measured $C_m/T|_{T\to 0}$ values within four decades, identifying three groups according their different behaviors: fermi liquids (FL), heavy fermions (HF) and very heavy fermions (VHF), see the text. For binary FL, see references in [7] and for ternary compounds see [8–11].

tiferromagnetic (AF) J_R between magnetic neighbors favored by some types of atomic coordinations. These peculiar group is included in the expanded phase diagram presented in Fig. 1 introducing a third axis.

II. DIFFERENT CLASSES OF HEAVY FERMIONS

Among the Ce and Yb compounds which do not order magnetically, the measured values of specific heat at $T \to 0$ ($C_m/T|_{T\to 0}$) cover more than three decades between the lowest reported value $\approx 8\,\mathrm{mJ/molK^2}$ in CeN and $CePd_7$ [7] and the highest $\approx 12\,\mathrm{J/molK^2}$ observed in $YbPt_2Sn$ [9], see Fig. 2. CeN and $CePd_7$ are characterized by a strong local ($4f$) and conduction states hybridization ($\propto J_K$) reflected in a large Kondo temperature [$T_K \propto \exp(-1/J_K)$]. On the weak hybridization range, the exemplary FL-HF with the highest $C_m/T|_{T\to 0}$ is $CeCu_6$ with a $\gamma = 1.6\,\mathrm{J/molK^2}$ [11] and $T_K \approx 10\,\mathrm{K}$. Its FL character is proved by the low temperature $\rho = AT^2$ dependence.

Between $1 \leq C_m/T|_{T\to 0} \leq 3\,\mathrm{J/molK^2}$ the most frequent behavior corresponds to compounds showing the characteristic NFL dependence: $C_m/T \propto -\ln(T/T_0)$ [1], where the energy scale T_0 plays a similar role than T_K. Coincidentally, the most representative NFL compounds show a $\rho \propto T$ dependence [12].

Recently, some Ce and a significant number of Yb compounds were found to clearly exceed the $C_m/T|_{T\to 0}$ values of NFL. These compounds can be labelled as Very-HF (VHF) because their $C_m/T|_{T\to 0}$ range between ≈ 5 and $\approx 12\,\mathrm{J/molK^2}$, see Fig. 2. The absence of magnetic order in these systems coincides with a huge increase of their spin correlations (sc) in the paramagnetic (pm) phase by decreasing temperature. Since at that range of temperature their magnetic behavior does not fit into the typical Curie-Weiss paramagnetism, they will be hereafter identified as 'sc-pm'. The strong increase of the density of magnetic excitations is reflected in a divergent power law dependence of $C_m(T)/T \propto 1/T^Q$, with exponents ranging between $1 \leq Q \leq 2$. This behavior is observed down to a temperature (T_{BN}) below which a clear deviation from the sc-pm behavior occurs due to an entropy bottleneck (BN) formation, to be described below.

Apart from the different values of $C_m/T|_{T\to 0}$ between NFL-HF and VHF, there are other distinctive properties indicating that these materials belong to different classes. An intrinsic difference is that in NFL the magnetic moments are increasingly quenched by Kondo effect and therefore located into the QC region, see the schematic phase diagram in the inset of Fig. 1. On the contrary, VHF exhibit robust moments with irrelevant Kondo effect, being the geometrical frustration responsible for the lack of magnetic order. As a consequence, their respective thermal scalings are different. While the $C_m(T)/T \propto -\ln(T/T_0)$ dependence of NFL was found to scale among different compounds through their T_0 temperatures [13], see Fig. 3a, the scaling among VHF compounds can be done through the exponents Q of their $1/T^Q$ dependencies. This feature is presented in Fig. 3b for five Yb-based examples using the following values: $Q = 1 \pm 0.2$ for $YbCu_{5-x}Au_x$ ($0.5 \leq x \leq 0.7$) [10], $Q = 1.4$ for $PrInAg_2$ [14], and $Q = 1.2$ for the $YbCu_4Ni$ [15] compound. Notably, all these compounds show a nearly coincident $C_m/T|_{T\to 0} \approx 7 \pm 0.7\,\mathrm{J/mol\ K^2}$ 'plateau' below a characteristic temperature T_{BN}.

There are other two compounds belonging to this VHF group: YbBiPt [16] and $YbCo_2Zn_{20}$ [17]. Al-

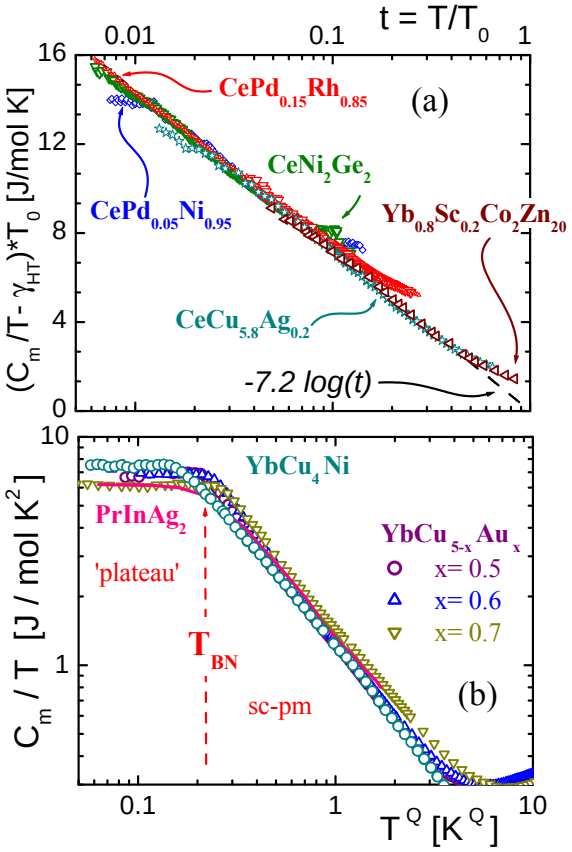

FIG. 3. (Color online) (a) Overlap of $C_m(t)$ dependencies of NFL-HF as a function of $-\ln(t)$ using a normalized temperature $t = T/T_0$ [13], where γ_{HT} accounts for the high temperature C_m/T contribution. (b) Power law overlap of five VHF as a function of normalized Q exponent of $1/T^Q$ in a double logarithmic representation. The 'sc-pm' region identifies the spin correlated-paramagnetic phase and T_{BN} the temperature of the onset of the $C_m(T)/T$ 'plateau' regime.

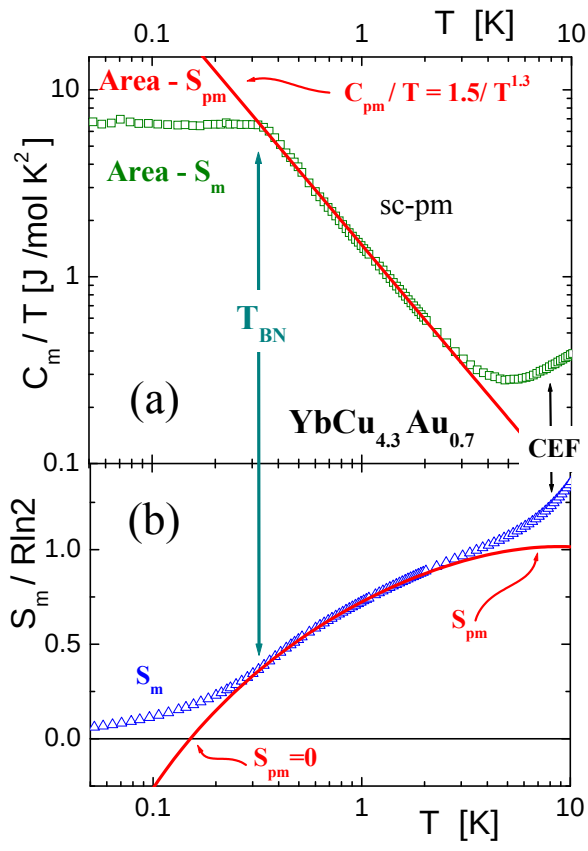

FIG. 4. (Color online) (a) Comparison between measured $C_m(T)/T$ and fitted $C_{pm}(T > T_{BN})/T$ dependencies in double logarithmic representation for a magnetically frustrated system [10]. S_m and S_{pm} represent the areas from which respective entropies are evaluated. (b) Thermal dependencies of those entropies, showing how $S_{pm} \to 0$ at $T > 0$. The value of $S_{pm}(T \to \infty)$ =Rln 2 is taken as reference for the doublet GS. CEF indicates the excited crystal field levels contribution above about 3 K.

though they show the same $C_m/T|_{T\to 0}$ values, they are not included in Fig. 3b because their low energy crystal electric field (CEF) levels already contribute to $C_m(T)/T$ around 1 K with the consequent deviation from the $1/T^Q$ dependence in the sc-pm phase. Expect these two cases, all the compounds analyzed in this work own a well defined doublet GS. Notably, the recently studied Sc-doped $YbCo_2Zn_{20}$ [18] system also fits into the NFL scaling presented in Fig. 3a for 19% of Sc content, with the record low value of $T_0 = 1.2$ K, whereas the low temperature contribution of the first excited CEF doublet is reflected in the large $\gamma_{HT} = 1.1$ J/molK^2 term. This supports the vicinity of the parent compound to a QC-point as discussed in Ref.[18].

III. THERMODYNAMIC ANALYSIS OF THE $S_m(T)$ TRAJECTORY

A. Origin of the $C_m/T|_{T\to 0}$ upper limit: Entropy bottlenecks

Since these systems are inhibited to order magnetically because of their frustrated character, spin correlations develop remarkably decreasing temperature in the sc-pm phase. As a consequence, the density of magnetic excitations ($\propto C_{pm}/T$) grows following a power law, as depicted in Fig. 4a for the exemplary system $YbCu_{4.3}Au_{0.7}$, that extrapolates to a mathematical singularity at $T = 0$. Therefore, a change of behavior is expected at finite temperature (hereafter

T_{BN}) in order to escape such unphysical point. The question arises why this change of regime occurs at certain characteristic temperature T_{BN} and how is its value established. To attempt to answer these questions one should take into account the relevance of the third law of thermodynamics in real systems at the $T \to 0$ limit.

In order to analyze how the third law (shortly expressed as $S_m(T)|_{T\to 0} \geq 0$) intervenes in determining the ground state (GS) of these VHF, the $C_m(T)/T$ dependence of the magnetically frustrated $YbCu_{4.3}Au_{0.7}$ [10] is chosen. In its pyrochlore-type structure the Yb-magnetic moments are located in tetrahedral vertices inhibiting magnetic order due a 3D geometric frustration. This property guarantees that no condensation of degrees of freedom occurs by magnetic order induced via standard magnetic interactions. In fact, no traces of order were detected in this system below T_{BN} by spectroscopic measurements [19]. In Fig. 4a one may appreciate that $C_m(T > T_{BN})/T$ increases obeying the power law dependence $\propto 1.5/T^{1.3}$ which, below $T_{BN} = 350\,\mathrm{mK}$, transforms into a 'plateau' with $C_m/T|_{T\to 0} \approx 6.5\,\mathrm{J/mol\,K^2}$. This plateau was obtained after subtracting the nuclear contribution of Yb atoms from the total measured specific heat [10].

The area label as Area-S_{pm} in Fig. 4a represents the entropy computed as $S_{pm} = \int 1.5/T^{1.3} \times dT$ for an heuristic system which does not change its C_{pm}/T dependence at T_{BN} and clearly exceed the 'Rln 2' physical limit for a doublet GS. On the contrary, the entropy extracted from the measurement as $S_m = \int C_m/T \times dT$, represented by Area-$S_m$, reveals that the diverging increase of $C_m(T > T_{BN}/T$ towards low temperature runs across an 'entropy bottleneck' (BN) [20] that compels it to change trajectory. This means that the change of $C_m(T)/T$ at $T = T_{BN}$ occurs because the system is constraint to not overcome the $S_m = R\ln 2$ value.

The comparison between $S_{pm}(T)$ and $S_m(T)$ trajectories is included in Fig. 4b. Since this analysis corresponds to a doublet GS, the $R\ln 2$ upper limit at high temperature is taken as the reference value. Notice that the contribution of the exited CEF levels to $C_m(T)$ ($S_m(T)$) only occurs above about $T = 3\,\mathrm{K}$. This comparison shows that both entropy trajectories match very well within the $0.3 \geq T \geq 2\,\mathrm{K}$ range. However, while $S_m(T < 0.3\,K)$ turns pointing to the expected $S_m|_{T\to 0} = 0$ limit, $S_{pm}(T)$ becomes zero a finite temperature (at $T \approx 0.17\,\mathrm{K}$ in this case) and keeps decreasing into negative values. It is clear that below $T = T_{BN}$ the third law imposes another trajectory to $S_m(T)$, which departs from $S_{pm}(T)$ in order to not overcome the physical limit of $S_m|_{T\to 0} = 0$. A relevant aspect of this change of trajectory for $S_m(T)$ arises from the fact that it is not driven by magnetic interactions but by the thermodynamic constraint: $S_m|_{T\to 0} \geq 0$.

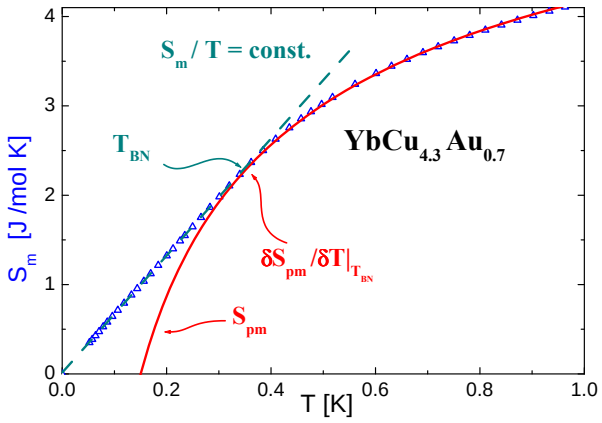

FIG. 5. (Color online) Analysis of the thermodynamic condition producing the entropy deviation from the sc-pm trajectory. Continuous curve: $S_{pm}(T)$, dashed line: S_m/T = constant.

B. Conditions to deviate from the sc-pm behavior

Once the origin of the change of regime was discussed, one should trace the thermodynamic conditions able to split $S_m(T)$ and $S_{pm}(T)$ trajectories at $T = T_{BN}$. For such a purpose we focus on $S_m(T_{BN})$ and $S_{pm}(T_{BN})$ coincidences. Looking at the same frustrated system $YbCu_{4.3}Au_{0.7}$, one may see in Fig. 5 that at T_{BN} the entropy derivative $\partial S_m/\partial T$ ($= \partial S_{pm}/\partial T$) coincides with the $S_m(T < T_{BN})/T$ ratio that extrapolates to $S_m|_{T\to 0} = 0$. Then, taking into account that $\partial S_m/\partial T \equiv C_m/T$, one finds that $C_m/T_{BN} = S_m/T_{BN}$ and therefore $S_m = C_m$ at that temperature.

Since the specific heat is defined as $C_m \equiv \partial E_m/\partial T$, where E_m is the magnetic enthalpy, the $S_m = C_m$ equality can be written as: $S_m - \partial E_m/\partial T = 0$. This expression coincides with the Planck's potential: $\Phi = S - E/T$ [21] provided that $\partial E_m/\partial T = E_m/T$, which is the case of the so-called 'plateau' regime of the VHF showing $C_m/T|_{T\to 0} = \text{const}$. That property fulfils the $\Phi = S_m - E_m/T = 0$ condition. Another relationship that characterizes this change if regime can be extracted from $\partial S_m/\partial T = S_m/T$ writing $\partial S_m/S_m = \partial T/T$. This implies that at $T = T_{BN}$ entropy and temperature (i.e. the thermal energy) change with the same ratio like in a sort of Grueneisen ratio: $\partial \ln S_m/\partial \ln T = 1$.

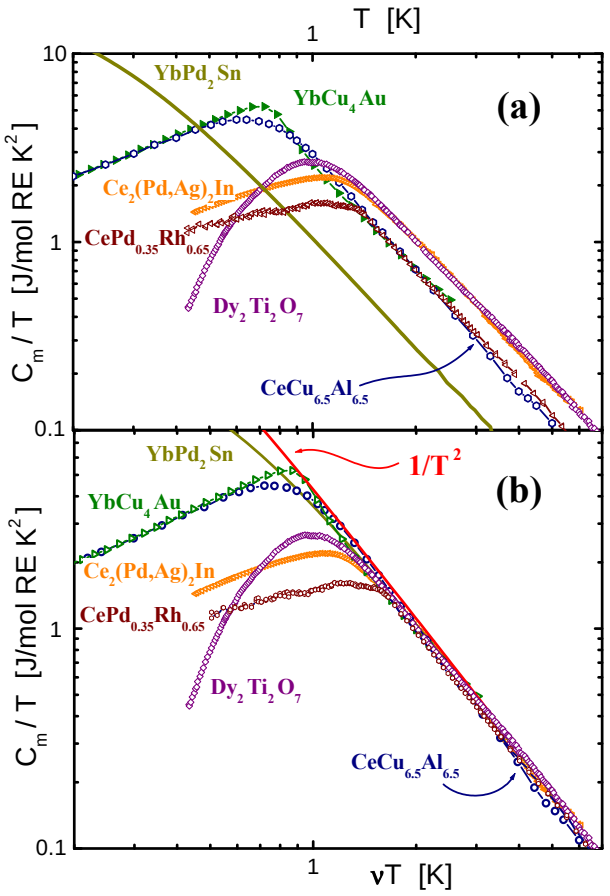

FIG. 6. (Color online) (a) Compounds with $C_m(T)/T$ maxima at $T \approx 1\,\mathrm{K}$ and the same power law dependence in their 'sc-pm' phases, after [26, 28]. Notice the double logarithmic representation and the mass normalization to a single rare earth (RE) atom. (b) Same compounds scaled by normalizing their respective temperatures with a factor ν, taking $Dy_2Ti_2O_7$ and $Ce_2(Pd_{0.5}Ag_{0.5})_2In$ as reference. A $1/T^2$ function is included to show the coincident dependence of these compounds.

C. Other cases with similar thermal C_{pm}/T dependencies

In order to recognize whether this 'entropy bottleneck' effect only occurs in the VHF with a $C_m/T|_{T\to 0}$ 'plateau' below T_{BN} or it is a general property, the same analysis is applied to a number of compounds collected in Fig. 6a which are inhibited to order magnetically. The figure contains some geometrically frustrated cases, like the 3D-pyrochlores $YbCu_4Ni$ and $Dy_2Ti_2O_7$ spin-ice [22] and the 2D $Ce_{2.15}(Pd_{0.5}Ag_{0.5})_{1.95}In_{0.9}$ [23], hereafter quoted as $Ce_2(Pd_{0.5}Ag_{0.5})_2In$ for simplicity. The latter system shows on-plane triangular coordination between Ce-nearest-neighbors in the Mo_2B_2Fe-type structure. A striking feature observed in all the mentioned systems is the nearly coincident power law dependence $C_m/T \propto 1/T^Q$ in the respective 'sc-pm' phases.

To explore the ampleness of this peculiar dependence besides frustration phenomena, other systems like: $YbPt_2Sn$ [9], $CeCu_{6.5}Al_{6.5}$ [25] and $CePd_{0.35}Rh_{0.65}$ single crystal [26] are included into this comparison because they show the same $C_m/T \propto 1/T^2$ dependence. Although the competition between the first-J_1 and second-J_2 neighbor magnetic exchange interactions may cause frustration in simple structures, the case of $CePd_{0.35}Rh_{0.65}$ seems to escape to that pattern because it was actually investigated in the context of a QC regime [27]. This supports one of the main points of the present analysis: the change in the $S_m(T)$ trajectory is due to thermodynamic constraints independently of the reason why magnetic order is inhibited. In other words, the lack of magnetic order down to very low temperature provides the conditions for the entropy-bottleneck occurrence.

Besides the coincident property of all systems included in Fig. 6a, that their $C_m(T > T_{BN})/T$ dependencies is described with the same heuristic formula $C_{pm}/T = D/(T^Q + E)$ [24] with $Q = 2 \pm 0.1$, one finds that $Dy_2Ti_2O_7$ and $Ce_2(Pd_{0.5}Ag_{0.5})_2In$ also coincide in all their fitting parameters: $D = 4.5\,\mathrm{J/mol}$ at. and $E = 0.3\,\mathrm{K}^2$ [23]. These systems do not show the VHF-plateau behavior because once reached the entropy-bottleneck conditions they access to some alternative minima of their free energy, which is evidenced by the decrease of their $C_m/T|_{T<T_{BN}}$.

As a consequence of their common power law dependence, these compounds can be scaled by a simple normalization of their D_ν coefficients: $D_\nu = \nu D$, taking as (arbitrary) reference the coincident $D = 4.5\,\mathrm{J/mol\,RE}$. value of $Dy_2Ti_2O_7$ and $Ce_2(Pd_{0.5}Ag_{0.5})_2In$, see Fig. 6b. In this comparison, the $C_m(T)/T$ properties of $YbPt_2Sn$ merit some comment because it coincides with some characteristics of this group but it differs from others. Together with its homologous $YbPt_2In$ [9], its $C_{pm}(T)/T \propto 1/T^2$ dependence coincides with the common $Q \approx 2$ exponent of other compounds despite showing the lowest temperature maximum of $C_m(T)/T$. This feature supports the fact that the underlying mechanism responsible for the entropy-bottlenecks formation does not depend of an energy scale but reflect a general thermodynamic property. Besides that, these $YbPt_2X$ compounds show that the $\approx 7\,\mathrm{J/molK}^2$ value observed in the 'plateau' group is not an upper limit for $C_m/T|_{T\to 0}$ but a characteristic of VHF.

The coincident $Q \approx 2$ value observed in the power law thermal dependence of the five rare earth based compounds collected in Fig. 6 clearly suggests that

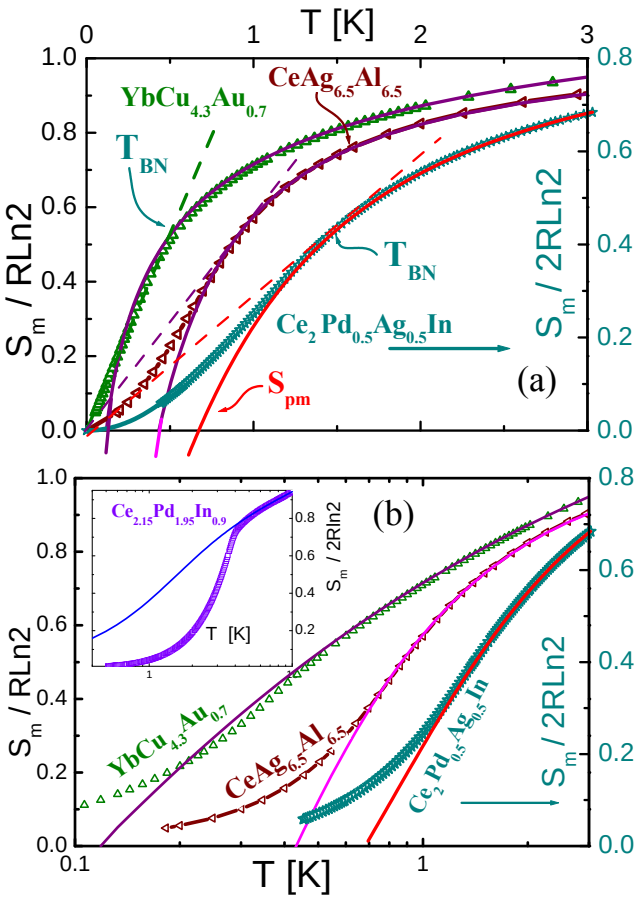

FIG. 7. (Color online) a) $S_m(T)$ dependencies of three compounds showing their respective $S_{pm} = 0$ extrapolations at $T > 0$ and respective S_m/T (dashed) lines defining T_{BN}. b) Same entropies dependencies in a log(T/K) representation compared (see the inset) with that of a standard ferromagnetic compound.

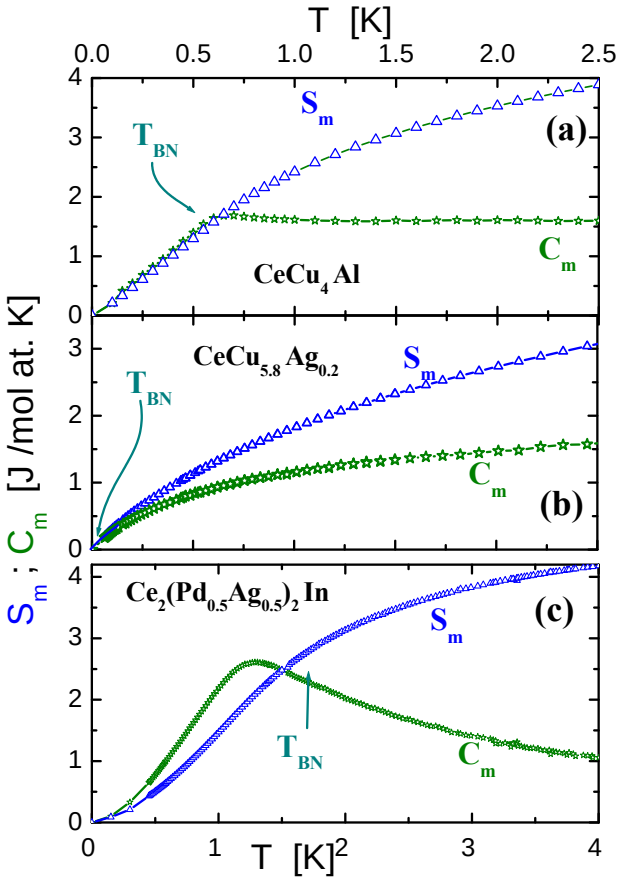

FIG. 8. (Color online) Comparison of $S_m(T)$ and $C_m(T)$ dependencies for three different types of GS: (a) a 'plateau' type with $T_{BN} \approx 0.6\,\mathrm{K}$, data after [30],(b) the case of a NFL [32], where $\Phi(T) = 0$ occurs at $T_{BN} = 0$, and (c) a 2D frustrated system showing a $C_m(T)/T_{max}$ at $\approx 1\,\mathrm{K}$, data after [23].

some common physics underlies in their 'sc-pm' behavior. Although power law dependencies for C_m/T are frequently reported in model predictions, the exponents use to be much smaller [1] than the observed. Nevertheless, a $Q = 2$ exponent was reported [29] to describe the thermal properties of Kondo type systems assuming a uniform distribution of T_K between 0 and a cut-off temperature with a $C_m/T \propto 1/(T^2 + T_K^2)$ dependence. However, mimicking T_K as the spin fluctuation energy of the frustrated-moment orientation in a sort of spin-liquid scenario, that expression nicely fits the reported experimental results.

D. Comparison between different entropy behaviors

Regarding the thermal dependence of the entropy, the same discussion performed in Fig. 4 about the change of trajectory at T_{BN} can be applied to these compounds, see Fig. 7a. Two representative cases are included in the figure: $Ce_2(Pd_{0.5}Ag_{0.5})_2In$ and $CeCu_{6.5}Al_{6.5}$, and compared with $YbCu_{4.3}Au_{0.7}$ already analyzed in Fig. 4 as a member of the 'plateau' group. Each $S_{pm}(T)$ dependence is computed as $S_{pm} = \int C_{pm}/T \times dT$, with respective $C_{pm}(T > T_{BN})/T = 1.46/T^{1.3}$ for $YbCu_{4.3}Au_{0.7}$, $= 9.1/(T^2 + 0.35)$ for $Ce_2(Pd_{0.5}Ag_{0.5})_2In$ and $= 3/T^2$ for $CeCu_{6.5}Al_{6.5}$. As it can be appreciated, all these $S_{pm}(T)$ trajectories cross the $S_m = 0$ axis at finite

temperature because $S_{pm}|_{T\to 0}$ extrapolates to the unphysical value $S_{pm}|_{T=0} < 0$.

Focusing to the actual value of S_m at T_{BN}, it is evident from Fig. 7a that $S_m(T_{BN}) \approx 1/2R\ln 2$. Within a significantly low dispersion, this observation includes the $CePt_2X$ compounds [9] and frustrated systems like $Ce_2(Pd_{0.5}Ag_{0.5})_2In$ and $Dy_2Ti_2O_7$. Interestingly, the $Dy_2Ti_2O_7$ spin-ice fits better into this systematic once the Pauling's residual entropy $S_0 = (1/2)R\ln(3/2)$ [38] is included into the 'total' $S_{tot} = S_m + S_0$.

In Fig. 7b the same picture is shown in a 'log(T/K)' representation in order to better distinguish the detachment between measured $S_m(T)$ and computed $S_{pm}(T)$ below $T = T_{BN}$. Interestingly, in $YbCu_{4.3}Au_{0.7}$ the S_m/T slope is slightly lower than the $\partial S_{pm}/\partial T$ around T_{BN} like as a reminiscence of a second order transition. Such a small effect is within the scale of eventual composition inhomogeneities at the surface of these poly-crystalline samples. As an inset in Fig. 7b, the case of the ferromagnet $Ce_{2.15}Pd_{1.95}In_{0.9}$ [31] is included for comparison. This magnetically ordered compound was selected because it shows a well defined $C_m(T_C)$ jump at relatively low temperature $T_C = 4.1\,\mathrm{K}$. It is evident that in this case the corresponding paramagnetic $S_{pm}(T > T_C)$ extrapolation below T_C remains above the measured $S_m(T < T_C)$ values, in clear contrast with the not ordered compounds. One should notice that the $\partial^2 S_m/\partial T^2$ derivative show an inflection point at $T = T_{BN}$ whereas at $T = T_C$ there is a discontinuity.

To check the applicability of the $C_m = S_m$ equality in a wider range of behaviors it is illustrative to compare the $C_m(T)$ and $S_m(T)$ dependencies in other systems that do not order magnetically but having GS of different nature. In Fig. 8a the stoichiometric compound $CeCu_4Al$ with a $T_{BN} \approx 0.6\,\mathrm{K}$, [30] is included as another example showing $C_m/T|_{T\to 0}$ constant and thence a coincident $C_m(T)$ and $S_m(T)$ below T_{BN}. Interestingly, as it is depicted in Fig. 8b the NFL $CeCu_{5.8}Ag_{0.2}$ [32] reaches the $C_m(T) = S_m(T)$ equality at $T = 0$ with consequent $T_{BN} = 0$. Due to their $C_m \propto -T \times \ln(T/T_0)$ dependencies the $C_m(T) - S_m(T)$ difference is expected to increase linearly with temperature. $CeCu_{5.8}Ag_{0.2}$ was chosen as a NFL exemplary system because it shows the largest measured value $C_m/T = 3\,\mathrm{J/mol\,K^2}$ at $T = 60\,\mathrm{mK}$, see Fig. 2. In spite of this, it does not reach the values of VHF even at $T \to 0$ because it shows a slight downwards deviation that extrapolates to $C_m/T|_{T=0} < 4\,\mathrm{J/mol\,K^2}$. Fig. 8c includes an example of a 2D frustrated system $Ce_2(Pd_{0.5}Ag_{0.5})In$ [23]. As expected from the analysis performed in Fig. 7a, the $C_m = S_m$ equality occurs where $C_m(T)/T$ deviates from the sc-pm regime described by the $\propto 1/T^2$ dependence. This temperature is close but not exactly at the maximum of $C_m(T)$. A replica of this behavior is obtained for the $Dy_2Ti_20_7$ spin-ice. This comparison supports the conclusion that the entropy-bottleneck is a general effect occurring in systems not able to reach magnetic order.

IV. THERMODYNAMIC BEHAVIOR AT $T \leq T_{BN}$

In order to gain insight into the peculiar behavior of these systems, one should focus on the two main questions arising from the observed phenomenology that mostly concerns the change of regime at $T = T_{BN}$ and the nature of the ground state beyond the entropy-bottleneck. Although the usual Kondo scenario, able to explain the lack of magnetic order can be discarded in these systems [33], in the range of temperatures where the entropy-bottlenecks occur ($T_{BN} \leq 1\,\mathrm{K}$) quantum fluctuations play an important role in the thermodynamic equilibrium because they may overcome thermal fluctuations [24].

According to a recent $'QK'$ phase diagram which includes frustration as a tuning parameter ($'Q'$), competing with Kondo effect ($'K'$) to define the GS of HF materials [34], the frustrated systems analyzed in this work can be placed on the 'spin liquid' (SL) side. Although that schematic phase diagram was proposed for antiferromagnetic (AFM) order (specifically related to Shastry-Shutherland lattice formation) as a wider concept it might include any possible type of order parameter. The fact that $Ce_2(Pd_{0.5}Ag_{0.5})_2In$ [23] is related to the Shastry-Shutherland lattice behavior of Ce_2Pd_2Sn [35] indicates that different GS of similar energies may become accessible, being the AFM order one of those possibilities. One should remind that AFM-J_R interactions and geometrical factors are basic ingredients to inhibit magnetic order through frustration effects.

A. Characteristics of the T_{BN} transition

In Fig. 9a the $C_m(T)$ dependence of other three systems are presented to show the effect of the entropy-bottleneck through an alternative picture. From the $C_m(T > T_{BN}) \approx$ const. behavior, it is evident that it would extrapolate to a non-physical $C_m \neq 0$ at $T = 0$ unless a change trajectory occurs once the $S_m = C_m$ equality is reached. The small jump at T_{BN} was already attributed to possible grains-surface contribution in poly-crystalline samples.

Since the change of regime occurs without a $C_m(T)$

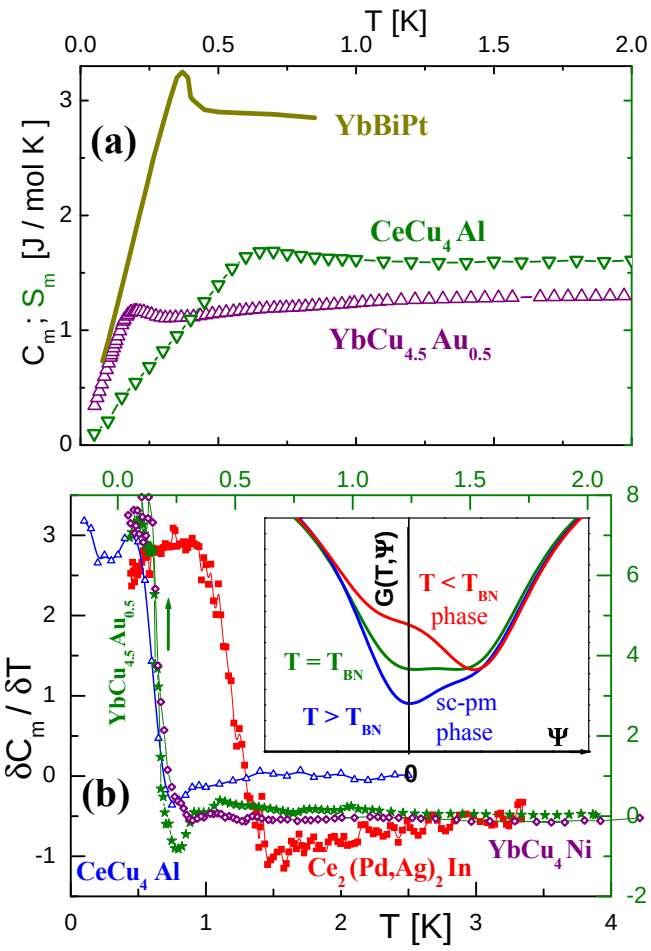

FIG. 9. (Color online) (a) Three illustrative cases: YbBiPt [16], CeCu4Al [30] and Yb $Cu_{4.5}Au_{0.5}$ [10], showing how $C_m(T \to 0) > 0$ before the entropy-bottleneck in reached. (b) $\partial C_m/\partial T$ derivative of some studied compounds showing a discontinuity at $T = T_{BN}$. Inset: isothermal $G(\Psi)$ representations for three different temperatures including a broad minimum at $T = T_{BN}$, after [39].

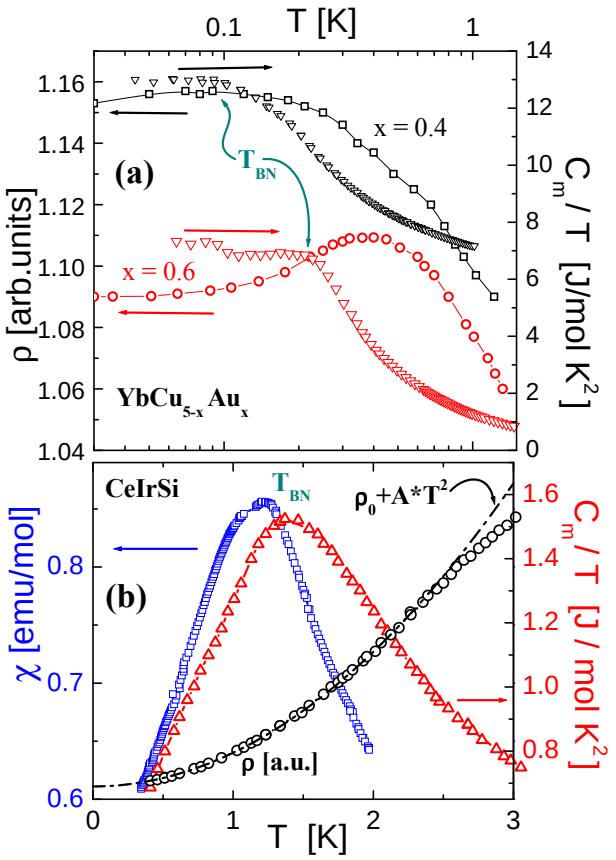

FIG. 10. (Color online) Continuous formation of a coherent GS indicted by electrical resistivity of systems belonging to: (a) the group showing a $C_m/T|_{T\to 0}$ 'plateau' [10, 41] and (b) to those with the C_m/T maximum at $T_{BN} \approx 1\,\mathrm{K}$, after [44].

jump, the following scenario can be proposed: the minimum of the free energy of the sc-pm phase (G_{pm}) blurs out at T_{BN} because it is not workable anymore and the system is compelled to slide into any other energetically accessible $G(T)$-minimum. This description is schematically depicted in the inset of Fig. 9b [39] as a $G_{pm}(\Psi)$ dependence on the order parameter Ψ at different temperatures. This continuous creep along the $G(\Psi, T)$ surface is related to a higher order discontinuity of the $G(T)$ derivative, i.e. $\partial G^3/\partial^3 T$, that emerges as a discontinuity in $\partial C_m/\partial T$ of third order transition character [40], clearly fulfilled by the transitions collected in Fig. 9b.

Another evidence for the third order character of this transition is given by the entropy trajectory in the low temperature phase. As it is shown in the inset of Fig. 7b for the case of a model second order FM transition, $S_m(T) < S_{pm}(T)$ below T_C because a magnetic order parameter $\Psi(T < T_C)$ develops condensing the entropy extrapolated from $T > T_C$. On the contrary, in the systems presented in Fig. 7, $S_m(T) > S_{pm}(T)$ below T_{BN}. This difference is a direct consequence of the $\partial S_m^2/\partial^2 T$ discontinuity at $T = T_C$ respect to the inflection point at $T = T_{BN}$.

B. Nature of the ground state beyond the entropy bottleneck

Despite of the scarce thermodynamic information available at very low temperature, some relevant features can be observed in the systems showing the $C_m/T|_{T\to 0} \approx 7\,\mathrm{J/molK^2}$ 'plateau'. Among them,

the already mentioned absence of magnetic order confirmed in $YbCu_{5-x}Au_x$ down to 20 mK using μSR and NQR techniques [19] is significant. Coincidentally, coherent electronic scattering is evident in $\rho(T)$ from $T > T_{BN}$ in samples with $x = 0.4$ and 0.6 [41]. This behavior is compared with the establishment of the specific heat 'plateau' at T_{BN}, see Fig. 10a.

Similar $\rho(T)$ coherence effects are observed in $PrInAg_2$ around $T_{BN} \approx 250$ mK [14]. Interestingly, the doublet GS of this compounds is not of Kramer's character because of the integer $J = 4$ total angular moment of Pr. This indicates that the type of GS wave function is irrelevant in the formation of the entropy-bottlenecks, supporting the purely thermodynamic origin of this phenomenon. Also the magnetic susceptibility (χ) of $YbCo_2Zn_{20}$ confirms the lack of magnetic order below T_{BN} because its $\chi(T)$ dependence simply shows a broad maximum at $T \approx 300$ mK [42] and the formation of a coherent lattice state well above T_{BN} [18].

From these experimental evidences one may conclude that the GS of these compounds behave more likely as Fermi or Spin Liquids rather than long range J_R-like interacting moments. This means that the change occurring at T_{BN} is not driven by standard magnetic interactions. Taking into account that this phenomenon occurs at the mK range of temperature, dominated by quantum fluctuations, eventual tunnelling effect between states of equivalent energy may act as hopping mechanism. In that case the formation of a very narrow band-like of excitations, reflected in a very high and constant $C_m/T|_{T\to 0}$ value, may arise. However, to our knowledge, there is no specific experimental indication in the literature for any of these scenarios.

The absence of magnetic order was also confirmed in the exemplary spin-ice for the family of compounds showing a $C_m(T)/T$ anomaly at $T_{BN} \approx 1$ K by transverse-field μSR experiments in $Dy_2Ti_2O_7$ [43]. A coherent GS formation is also supported by $\rho(T)$ measurements in CeIrSi [44], where Ce-atoms coordination provides the geometrical condition for magnetic frustration. In this compound $\rho(T)$ obeys a $\rho = \rho_0 + A \times T^2$ dependence for $T \leq 2.4$ K which reveals a coherent electronic scattering, see Fig. 10b. This range of temperature fully covers respective $C_m(T)/T$ and $\chi(T)$ anomalies around $T_{BN} \approx 1.4$ K. The absence of magnetic order was also remarked in YbBiPt [16], with a considerably small T_K and a monotonous decrease of $\rho(T)$.

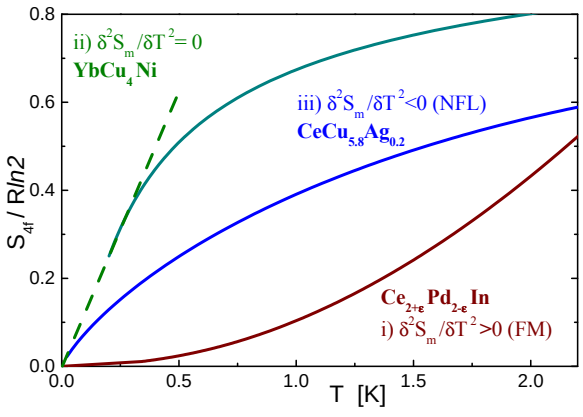

FIG. 11. (Color online) Different ways for $S_m|_{T\to 0}$ according to its second derivative $\partial^2 S_m/\partial T^2$.

C. Analysis of the thermal dependencies of the entropy at $T \to 0$ in real systems

Despite of the leafy literature devoted to the $S_m|_{T\to 0} \geq 0$ postulate, there is scarce information about the $S_m(T)$ derivatives approaching $T = 0$ [45]. Although the unattainability of that limit prevents any experimental approximation, the present knowledge of the $S_m(T)$ behavior of Ce- and Yb-based compounds not showing magnetic order allows to explore that field from a phenomenological point of view. This topic is becoming relevant because the efficiency of new cryo-materials for adiabatic demagnetization at very low temperature depends on how magnetic field affects the $S_m(T)$ and its slope, i.e. $C_m/T = \partial S_m \partial T$, at the proximity of $T = 0$.

Some interesting features can be extracted from the analysis of the possible trajectories of $S_m|_{T\to 0}$, schematically drown in Fig. 11 and formerly discussed in Ref.[46]. The three possible curvatures presented in the figure can be classified according to their second thermal derivatives $\partial^2 S_m/\partial T^2$: i) the positive ($> 0$) curvature corresponds to standard ordered systems acceding to a cooperative GS, represented by the FM compound $Ce_{2+\epsilon}Pd_{2-\epsilon}In$ [31], ii) the zero curvature ($= 0$) identifies to the group showing a 'plateau' in $C_m/T|_{T\to 0}$ and corresponds to a continuous density of excitations, like e.g. in FL. iii) The negative curvature (< 0) is characteristic of frustrated systems in the 'sc-pm' regime, which cannot extrapolate to $T = 0$ because it would end at a singularity. As a consequence, no experimental example can be quoted since real systems are compelled to modify their $S_m(T)$ trajectory at T_{BN}. The lowest temperature $\partial^2 S_m/\partial T^2|_{T\to 0} < 0$ curves are observed in NFL

compounds because their $C_m \propto -T \times \ln(T/T_0)$ dependence extrapolate to $C_m|_{T\to 0} = 0$, see the case of $CeCu_{5.8}Ag_{0.2}$ [32] in Fig. 8b. As mentioned before, this case corresponds to a $T_{BN} = 0$ scenario. The moderate increase of the entropy at the mK range produced by the extended energy range of magnetic excitations, $S_m(T) \propto T - T \times ln(T/T_0)$, allows the closest approach to $\partial^2 S_m/\partial T^2|_{T=0} < 0$. In Fig. 11, $CeCu_{5.8}Ag_{0.2}$ is taken as the exemplary system with a pure doublet GS because, in the case of $(Yb_{0.8}Sc_{0.2})Co_2Zn_{20}$ [18], the first excited CEF level already contributes to $S_m(T)$ within the temperature range of the figure. Interestingly, such Sc-doping is able to drive the $T_{BN} \approx 200\,\mathrm{mK}$ of Yb_2Zn_{20} down to zero as atomic disorder weakens the spin-correlations that reduces C_m/T above T_{BN} with the consequent shift of the entropy-bottleneck effect to lower temperature.

V. CONCLUSIONS

Along this work it was shown how the absence of magnetic order, inhibiting magnetic degrees of freedom to condensate into a singlet GS, can be profited to investigate the effects of the third law of thermodynamics in real materials. It can be observed how the enhanced paramagnetic correlations strongly increase the density of low energy excitations inducing the formation of VHF systems. Apart from the clear quantitative difference of $C_m/T|_{T\to 0}$ between VHF and NFL, respective power law and logarithmic thermal dependencies testify their distinct physical nature.

The divergent increase of this density of excitations collides with the limited amount of the paramagnetic degrees of freedom ($R\ln 2$ for a doublet GS) producing an entropy-bottleneck which becomes responsible for the change of the $S_m(T)$ trajectory. Such 'bottleneck' occurs in these systems because they are not able to access an ordered state when approaching the exhaustion of their degrees of freedom. Since this change in the $S_m(T)$ trajectory is not driven by standard magnetic interactions but by thermodynamic constraints, this process occurs though a continuous transition of third order character. The temperature at which the entropy-bottleneck occurs is associated to the $S_m = C_m$ equality.

Notably, among the compounds showing a constant $C_m/T|_{T\to 0}$ also coincident value $\approx 7 \pm 0.7\,\mathrm{J/molK^2}$ is measured. Despite of the dispersion observed in the T_{BN} values of these compounds, the convergent value of $C_m/T|_{T\to 0}$ seems to be a characteristic property which identifies the 'plateau' group whose. Whether this specific value has an underlying physical origin remains an open question. Besides that, the coherent regime observed in $\rho(T)$ around T_{BM} suggests a sort of FL or eventual SL behavior below that temperature. In standard FL, constant $C_m/T|_{T\to 0}$ and $\rho(T)$ coherence are related to a narrow electron band, that in the present scenario could be tentatively associated to a quantum tunnelling effect connecting levels of similar energy. This possibility requires to be confirmed by spectroscopic investigations because it would represent a singular case of a quantum GS that becomes accessible due to an entropy bottleneck.

These systems also allow to perform an empirical approach to the study of the entropy derivatives, showing that negative curvature ($\partial^2 S_m/\partial T^2 < 0$) has the best physical representation in NFL compounds, whose logarithmic dependencies of $S_m(T)$ and $C_m(T)$ place the $S_m = C_m$ equality at $T = 0$. Independently of their NFL or VHF character, the field dependence of S_m at the milikelvin range is the main parameter that characterizes the best materials for adiabatic demagnetization purposes.

It is evident that the recent generation of rare earth based compounds, exhibiting robust magnetic moments but inhibited to develop magnetic order, allows to explore the properties of exotic ground states within a region of temperature where the interplay between thermodynamic and quantum properties may trigger novel behaviors.

ACKNOWLEDGMENTS

The author is grateful to I. Curlik, M. Giovannini, T. Gruner, M. Deppe, E. Bauer, H. Michor, M. Reiffers, E-W Scheidt, A. Strydom and I. Zeiringer for allowing to access to original experimental results. This work was partially supported by projects: PIP-2014 Nr. 112-2013-0100576 of CONICET and SECyT 06/C520 of Univ. of Cuyo (Arg.).

[1] G.R. Stewart; Rew. Mod. Phys. **73** (2001) 797.
[2] H.v. Löhneysen, A. Rosch, M. Vojta, P. Wöfle; Rew. Mod. Phys. **79** (2007) 1015.
[3] G.K. White and P.J. Meeson, in *Experimental Techniqhes in Low-TemperaturePhysics*, Clarendon Press, Oxford, 2002.
[4] S. Doniach, Physica B & C **91** (1977) 231.
[5] M. Lavagna, C. Lacroix, M. Cyrot, Phys. Lett. 90A (1982) 210. and J. Phys. F 13A (1983) 1007.
[6] T. Vojta, Annalen der Physik **9** (2000) 403-440.

[7] J.G. Sereni, in *Low Temperature Specific Heat of Cerium Compounds*, Handbook on the Physics and Chemistry of Rare Earths, Eds. K.A. Cschneidner, Jr. and L. Eyring Elsevier Science Puhlishers B. V., Ch. 98, Vol.**15** (1991) 1.

[8] C. Gold, M. Uffinger, M. Herzinger, G. Eickerling, W. Scherer, H. Michor, E.-W. Scheidt; J. Alloys and compounds **523** (2012) 61.

[9] T. Gruner, D. Jang, A. Steppke, M. Brando, F. Ritter, C. Krellner, C. Geibel; J. Phys.: Condens. Matter **26** 485002 (2014) and D. Jang, T. Gruner, A. Steppke, K. Mistsumoto, C. Geibel, M. Brando; Mature Communications, ncomms9680 (2015).

[10] I. Curlik, M. Giovannini, J.G. Sereni, M. Zapotokova, S. Gabani, M. Reiffers; Phys. Rev. B **90** 224409 (2014).

[11] A. Amato, D. Jaccard,J. Flouquet,E. Lapierre,J.L. Tholence, R.A. Fisher, S.E. Lacy, J.A.Olsen and N.E. Phillips, J. Low Temp.Phys. 68 (1987) 371.

[12] See ref. [1] and G.R. Stewart; Rev. Mod. Phys. **78** 743 (2006).

[13] J.G. Sereni, C. Geibel, M. G-Berisso, P. Hellmann, O. Trovarelli, F. Steglich, Phys. B **230-232** (1997) 580.

[14] A. Yatskar, W.P. Beyermann, R. Movshovich, P.C. Canfield ; Phys. Rev. Lett. **77** (1996) 3637.

[15] A. M. Strydom, University of Johannesburg, South Africa, private communication, 2016.

[16] Z. Fisk, P.C. Canfield, W.P. Beyermann, J.D. Thompson, M.F. Hundley, H.R. Ott, E. Felder, M. B. Maple, M.A. Lopez de la Torre, P. Visani, C. L. Seamanet; . Phys. Rev. Lett. **67** (1991) 3310.

[17] M.S. Torikachvili, S. Jia, E.D. Mun, S.T. Hannahs, R.C. Black, W.K. Neils, D. Martien, S.L. Bud'ko, P.C. Canfield; PNAS **104** (2007) 9960.

[18] Y. Tokiwa, B. Piening, H.S. Jeevan, S.L. Budko, P.C. Canfield, P. Gegenwart; Sci. Adv. 2 (2016) e1600835.

[19] P. Carretta, R. Pasero, M. Giovannini, C. Baines; Phys. Rev. B **79** 020401(R) (2009).

[20] J.G. Sereni, in: *Magnetic Systems: Specific Heat*, Saleem Hashmi (editor-in-chief), Materials Science and Materials Engineering. Oxford: Elsevier; 2016. pp. 1-13; ISBN: 978-0-12-803581-8

[21] M. Planck, in *Treatise on Thermodynamics*, Dover Publications, Inc., 1926.

[22] Z. Hiroi, K. Matsuhira, M. Ogata; J. Phys. Soc. Japn. **72** (2003) 304545.

[23] J.G. Sereni, M. Giovannini, M. Gómez Berisso, F. Gastaldo; J. Phys. Cond. Matter, **28** (2016) 475601.

[24] J.G. Sereni, J. Low Temp. Phys. **149** (2007) 179.

[25] U. Rauchschwalbe , U. Gottwick, U. Ahlheim, H.M. Mayer, F. Stelich; J. Less Ccomm. Metals **111** (1985) 265.

[26] S. Hartmann, M. Deppe, N. Oeshler, N. Caroca Canales, J.G. Sereni, C. Geibel; J. Optoelectr. and Adv. Mat. **10** (2008) 1607.

[27] J.G. Sereni, T. Westerkamp, R. Kchler, N. Caroca-Canales, P. Gegenwart, C. Geibel; Phys. Rev. B **75** (2007) 024432.

[28] Refs. for compounds included in Fig. 6: $Dy_2Ti_2O_7$ [22]; $Ce_2(Pd_{0.5}Ag_{0.5})_2In$ [23]; $CeCu_{6.5}Al_{6.5}$ [25] and $YbCu_4Au$ [36].

[29] A.J. Schofield, Contemp. Phys. **40** (1999) 95.

[30] E. Bauer; Adv. Phys. **40** (1991) 417.

[31] J.G. Sereni, M. Giovannini, M. G-Berisso, A. Saccone, Phys. Rev. B **83** (2011) 064419.

[32] E.-W. Scheidt, D. Maurer, A. Weber,T. Götzfried, K. Heuser, S. Kehrein, R. Tidecks, Physica B **321** (2002) 133137.

[33] Remind that the case of $CePd_{0.5}Rh_{0.5}$ as an example of QC behavior is included to show that the change in the $S_m(T)$ trajectory is due to themodynamic constraints, independently to the cause of the lack of magnetic order.

[34] P. Coleman, A.H. Nevidomskyy; J. Low Temp. Phys. **161** (2010) 182-202.

[35] J.G. Sereni, M. Gmez Berisso, A. Braghta, G. Schmerber, J.P. Kappler; Phys. Rev. B **80** (2009) 024428.

[36] M. Galli, E. Bauer, St. Berger, Ch. Dusek, M. Della Mea, H. Michor, D. Kaczorowski, E.W. Scheidt, F. Marabelli; Physica B **312-313** (2002) 489.

[37] Unpublished results obtained from a single-crystal sample provided by S. Grigera, Universidad Nacional de La Plata, Argentina (2008).

[38] A.P. Ramirez, A. Hayashi, R.J. Cava, R.

[39] See for example J.G. Sereni; J. Low Temp. Phys. **179** 126 (2015).

[40] A.B. Pippard, in *Elements of classical Thermodynamics*, University Press, Cambridge, 1964.

[41] K. Yoshimura, T. Kawabata, N. Sato., N. Tsujii, T. Terashima, C. Terakura, G. Kido, K. Kosuge; J. of Alloys and Compounds **317318** (2001) 465.

[42] T. Takeuchi, M. Ohya, S. Yoshiuchi, M. Matsushita, F. Honda, R. Settai, Y. Onuki; J. Phys.: Conf. Series **273** (2011) 012059.

[43] S.R. Dunsiger, A.A. Aczel, C. Arguello, H. Dabkowska, A. Dabkowski, M.-H. Du, T. Goko, B. Javanparast, T. Lin, F. L. Ning, H.M.L. Noad, D.J. Singh, T.J. Williams, Y.J. Uemura, M.J.P. Gingras, G.M. Luke, Phys. Rew. Lett. **107** (2011) 207207.

[44] F. Kneidinge, Ph.D. Thesis, Technische Univertität Wien (2013), unpublished.

[45] J.P. Abriata, D.E. Laughlin, Progr. in Mat. Science, **49** (2004) 367.

[46] J.G. Sereni, Phil. Mag. **93** (2013) 409.